

Article

Baicalin ameliorates type 2 diabetes by modulating HIF-1 α -mediated oxidative stress and apoptosis: A network pharmacology and experimental study

Xudong Zhou^{1†}, Yanqiu You^{1†}, Chunhui Guo², Meng Gao², Zhiqiang Li¹, Jibing Chen^{2*}, Fujun Li^{2*}¹ Guangxi University, Nanning 530000, China² Ruikang Hospital Affiliated to Guangxi University of Chinese Medicine, Nanning 530000, China* **Corresponding authors:** Jibing Chen, jibingchen398@163.com; Fujun Li, lfjyyq@163.com

† These authors are co-first authors.

CITATION

Zhou X, You Y, Guo C, et al. Baicalin ameliorates type 2 diabetes by modulating HIF-1 α -mediated oxidative stress and apoptosis: A network pharmacology and experimental study. *Molecular & Cellular Biomechanics*. 2025; 22(5): 1881. <https://doi.org/10.62617/mcb1881>

ARTICLE INFO

Received: 14 March 2025

Accepted: 25 March 2025

Available online: 3 April 2025

COPYRIGHT



Copyright © 2025 by author(s). *Molecular & Cellular Biomechanics* is published by Sin-Chn Scientific Press Pte. Ltd. This work is licensed under the Creative Commons Attribution (CC BY) license. <https://creativecommons.org/licenses/by/4.0/>

Abstract: This study investigates baicalin, a flavonoid from *Scutellaria baicalensis*, as a multi-target therapeutic for type 2 diabetes mellitus (T2DM) through cellular experiments, network pharmacology, and molecular docking. Baicalin improves pancreatic β -cell viability, reduces reactive oxygen species (ROS), and attenuates apoptosis/senescence in methylglyoxal (MGO)-induced models. Network pharmacology identifies key targets including HIF-1 α , Bax, Bcl-2, and Caspase-3, while molecular docking confirms strong interactions with proteins like AKT1 and HIF-1 α , underlying antioxidative and anti-apoptotic mechanisms. Notably, baicalin's protective effects extend to molecular biomechanical pathways, potentially modulating extracellular matrix (ECM) remodeling and cytoskeletal dynamics. In T2DM, hyperglycemic stress disrupts ECM integrity and mechanotransduction signaling (e.g., integrin-MAPK axis), contributing to β -cell dysfunction. Baicalin's regulation of ECM components (e.g., collagen, fibronectin) and cytoskeletal proteins (e.g., actin polymerization) may restore cellular mechanical phenotypes, enhancing β -cell survival and insulin secretion. This biomechanical modulation aligns with exercise's benefits in T2DM, where physical activity improves ECM elasticity and mechanosignaling, complementing baicalin's antioxidative and anti-apoptotic actions. Our findings highlight baicalin as a novel therapeutic addressing both biochemical and biomechanical hallmarks of T2DM, suggesting a synergistic strategy combining baicalin with exercise to restore metabolic and mechanical homeostasis.

Keywords: type 2 diabetes mellitus; baicalin; oxidative stress; exercise; HIF-1 α ; network pharmacology; molecular docking

1. Introduction

The global prevalence of diabetes mellitus (DM) continues to demonstrate a concerning upward trajectory, positioning this metabolic disorder as one of the most pressing public health issues worldwide. Current statistics indicate that over half a billion adults (537 million) were diagnosed with diabetes in 2021, with modeling studies predicting a dramatic escalation to 783 million affected individuals within the next two decades [1]. The upward trend is strongly correlated with key determinants such as accelerated urban development, widespread adoption of sedentary behavior patterns, and the growing global burden of obesity-related health issues [2]. The disease spectrum of diabetes mellitus encompasses two major subtypes: Type 1 diabetes, resulting from autoimmune-mediated pancreatic β -cell dysfunction and subsequent insulin deficiency, and Type 2 diabetes, which dominates the epidemiological landscape with >90% of cases and manifests through insulin

resistance accompanied by progressive β -cell failure [3,4]. T2DM is a multifactorial disease influenced by genetic predisposition, environmental factors, and lifestyle choices. Chronic hyperglycemia, the hallmark of diabetes, leads to a cascade of metabolic dysfunctions, including oxidative stress, inflammation [5], and cellular damage, which contribute to the development of diabetic complications such as neuropathy [6], retinopathy [7], nephropathy [8], and cardiovascular diseases [9].

Oxidative stress represents a pivotal pathological mechanism in T2DM pathogenesis and its clinical sequelae, resulting from disproportionate ROS production overwhelming endogenous antioxidant defenses. The diabetic milieu, characterized by persistent hyperglycemia, promotes oxidative damage through several mechanisms: impaired mitochondrial electron transport chain function, upregulated polyol and hexosamine flux, and progressive AGEs formation, which synergistically drive excessive ROS production [10]. Elevated ROS levels mediate extensive oxidative damage to critical biomolecules, including membrane phospholipids, cellular proteins, and nucleic acids, triggering dysfunction of fundamental cellular processes and activation of apoptotic pathways [11]. Oxidative stress signaling is predominantly mediated by the Nrf2-ARE pathway, responsible for transcriptional activation of antioxidant defense mechanisms, and the NF- κ B pathway, which coordinates cellular inflammatory responses through regulation of cytokine production and immune modulation [12,13]. Additionally, ROS activates stress-sensitive pathways such as the p38 mitogen-activated protein kinase and c-Jun N-terminal kinase pathways [14], further promoting apoptosis and insulin resistance. The interplay between oxidative stress and apoptosis is particularly critical in diabetes, as it contributes to the loss of Ins-1 and the dysfunction of insulin-sensitive tissues. For instance, ROS-induced activation of the intrinsic apoptotic pathway involves the upregulation of pro-apoptotic proteins such as Bax and Caspase-3, while downregulating anti-apoptotic proteins like Bcl-2 [15]. Furthermore, oxidative stress stabilizes hypoxia-inducible factor-1 α (HIF-1 α) [16], a transcription factor that regulates cellular responses to hypoxia and is implicated in diabetic complications such as retinopathy and nephropathy.

Additionally, oxidative stress orchestrates a complex interplay with molecular biomechanical remodeling. Excessive ROS not only damage lipids, proteins, and DNA but also disrupt extracellular matrix homeostasis and cytoskeletal dynamics [17], creating a bidirectional pathogenic loop. Mechanistically, ROS promote fibrosis by upregulating collagen deposition and downregulating matrix metalloproteinases, stiffening pancreatic islets and impairing β -cell mechanosensitivity [18]. Concurrently, ROS-induced actin cytoskeleton disorganization compromises insulin granule trafficking and β -cell shape maintenance, exacerbating secretory dysfunction [19]. This biomechanical dysregulation reciprocally amplifies oxidative stress: rigidified ECM activates integrin-MAPK signaling, triggering ROS overproduction, while cytoskeletal abnormalities blunt Nrf2 nuclear translocation, further attenuating antioxidant responses [20]. This redox-mechanical crosstalk drives β -cell loss through dual pathways: direct ROS-mediated apoptosis via Bax/Bcl-2 imbalance and indirect mechanotransduction impairment via ECM stiffening [20]. Collectively, these findings highlight the necessity of therapeutic strategies targeting both biochemical and biomechanical hallmarks of T2DM.

In recent years, natural compounds have gained significant attention for their

potential in managing diabetes and its complications. BA, a bioactive flavonoid derived from the roots of *Scutellaria baicalensis*, has emerged as a promising candidate due to its anti-inflammatory, antioxidant, and anti-apoptotic properties [21]. BA is known to modulate multiple signaling pathways, including the Nrf2/ARE pathway [22], which enhances cellular antioxidant defenses, and the PI3K/Akt pathway [23], which promotes cell survival and insulin sensitivity. Moreover, BA has been shown to inhibit NF- κ B activation [24], thereby reducing inflammation and oxidative stress. In traditional Chinese medicine, BA is often used in combination with other herbs to treat diabetes and its complications. For example, the Huang-Lian-Jie-Du-Tang formula, which contains BA, has been reported to improve insulin sensitivity and reduce blood glucose levels in diabetic models [25]. Similarly, the Gegen Qinlian decoction, another BA-containing formulation, has demonstrated efficacy in alleviating diabetic nephropathy by suppressing oxidative stress and inflammation [26]. These studies highlight the therapeutic potential of BA in diabetes management, particularly when used as part of a multi-component approach.

While extensive research has highlighted the therapeutic benefits of BA-containing formulations, the specific mechanisms underlying the action of pure BA in T2DM remain insufficiently characterized. Furthermore, recent findings suggesting dose-dependent cytotoxicity of BA underscore the need for rigorous evaluation of its safety profile and therapeutic window. To address these critical gaps, we conducted a systematic investigation of low-dose BA in an MGO-induced diabetic cell model, focusing on its antioxidant and anti-apoptotic properties. Utilizing an integrated strategy that combines computational approaches (network pharmacology and molecular docking) with experimental validation, we elucidated BA's interactions with key molecular targets, including P53, Bax, Bcl-2, Caspase-3, and HIF-1 α . Our study comprehensively evaluated BA's effects on cellular viability, senescence, oxidative stress, and apoptosis. These findings offer novel mechanistic insights into BA's protective role in diabetic conditions and highlight its potential as a safe and effective therapeutic agent for diabetes and its complications.

This study not only addresses a significant gap in the current understanding of BA's role in diabetes but also contributes to the broader field of natural product research by demonstrating the importance of dose optimization and mechanistic exploration in the development of plant-based therapies. By elucidating the molecular pathways involved in BA's effects, we hope to pave the way for future clinical studies and the development of BA-based interventions for T2DM.

2. Materials and methods

2.1. Chemicals

The experimental materials, including FBS, penicillin-streptomycin, and trypsin-EDTA, were procured from Saiwei'er Biotechnology (Nanning, China). Baicalin (BA) and methylglyoxal (MGO) were supplied by MedChemExpress (MCE, Monmouth Junction, NJ, USA), while Ins-1 pancreatic β -cells were sourced from Cyagen Biosciences (Guangzhou, China). Cell viability was measured using the Cell Counting Kit-8 (CCK-8) supplied by Saiwei'er Biotechnology. Cellular senescence was identified through-galactosidase staining with the Senescence-Galactosidase Staining

Kit from Saiwei'er. The quantification of intracellular reactive oxygen species (ROS) was carried out using the ROS Detection Kit by Saiwei'er. Additionally, apoptosis was evaluated using the Annexin V-FITC/PI Apoptosis Detection Kit provided by Saiwei'er.

2.2. Cell experiments

2.2.1. Cell viability assay (CCK-8)

Cell viability was assessed utilizing the CCK-8 assay. The experimental design for cellular treatments was structured as follows: (1) MGO exposure at concentrations spanning 0 to 4000 M for 12, 24, and 48 h; (2) BA treatment at concentrations of 0 to 400 M for 12, 24, and 48 h; (3) initial exposure to 1000 M MGO for 12 h, followed by treatment with BA (0 to 50 M) for an additional 12 h; (4) pretreatment with BA at concentrations from 0 to 50 M for 12 h, followed by 1000 M MGO for a further 12 h; and (5) concurrent treatment with 1000 M MGO and BA (0 to 50 M) for 12 h. After the respective treatments, 100 μ L of phenol red-free medium and 10 μ L of CCK-8 reagent (MCE, Shanghai, China) were added to each well. The plates were incubated at 37 °C for 1.5 h, after which absorbance was measured at 450 nm using a Pynamica microplate reader (Pynamica, Switzerland). The viability of cells was expressed as a percentage of the untreated control group.

2.2.2. Measurement of intracellular ROS

The experimental groups were designed as follows: (1) control group (untreated), (2) 1000 μ M MGO-induced group, (3) 1000 μ M MGO + 10 μ M BA treatment group, (4) 1000 μ M MGO + 20 μ M BA treatment group, and (5) 1000 μ M MGO + 50 μ M BA treatment group. This grouping scheme was consistently applied to all subsequent experiments.

To determine ROS levels, Ins-1 cells were seeded at 50,000 cells per well in 96-well plates and allowed to attach overnight. Following application of the respective treatments for each experimental group, the cells were incubated with the fluorescent probe 2',7'-dichlorofluorescein diacetate (DCFH-DA), diluted 1:100 in serum-free RPMI-1640, for 30 min at 37 °C in the dark. Excess probe was discarded after two PBS washes. The fluorescence intensity, reflecting the intracellular ROS content, was monitored and recorded with a Leica inverted fluorescence microscope (Leica, Germany).

2.2.3. Assessment of cell senescence by β -galactosidase staining

Ins-1 cells were placed at a density of 1 million per well on coverslips in 6-well plates. After completing the treatment sequence, the cells were flushed with PBS, then prepared for fixation and staining with the Senescence β -Galactosidase Staining Kit (Cell Signaling Technology), in line with the kit's instructions. The detection of senescent cells was indicated by a blue coloration observed through an Olympus biological microscope (Olympus, Japan).

2.2.4. Flow cytometry analysis of cell apoptosis

Cells were seeded in 6-well plates at 1×10^6 cells/well, treated, then harvested and washed with PBS. Transferred to 100 μ L binding buffer with 5 μ L Annexin V-FITC and 5 μ L PI, incubated in the dark at RT for 15 min. Post-incubation, diluted

with 400 μ L buffer and analyzed on a Beckman Coulter flow cytometer.

2.2.5. Quantitative real-time PCR (qPCR)

RNA extraction from Ins-1 cells was performed using TRIzol reagent, followed by cDNA synthesis with a reverse transcription kit. Quantitative PCR (qPCR) was conducted using SYBR Green Master Mix on a real-time PCR machine, employing gene-specific primers for P53, Bax, Bcl-2, Caspase-3, HIF-1 α , and GAPDH as a housekeeping gene. The primer sequences for the target genes were as follows: Hif1a (forward: 5'-ACCGTGCCCTACTATGTTCG-3', reverse: 5'-GCCTTGTATGGGAGCATTAACCT-3'), Casp3 (forward: 5'-CTGGACTGCGGTATIGAGACA-3', reverse: 5'-CGGGTGCGGTAGAGTAAGC-3'), BAX (forward: 5'-TGAAGTGGACAACAACATGGAG-3', reverse: 5'-AGCAAAGTAGAAAAGGGCAACC-3'), BCL2 (forward: 5'-CATGTGTGTGGAGAGCGTCAA-3', reverse: 5'-CAGCCAGGAGAAATCAAACAGA-3'), P53 (forward: 5'-GGAGGATTCACAGTCGGATATG-3', reverse: 5'-TGAGAAGGGACGGAAGATGAC-3'), and GAPDH (forward: 5'-CATGAGAAGTATGACAACAGCCT-3', reverse: 5'-AGTCCTTCCACGATACCAAAGT-3'). Relative mRNA expression levels were determined using the $2^{-\Delta\Delta Ct}$ method, with GAPDH as the internal standard.

2.2.6. Statistical analysis

The results are expressed as mean \pm SD from at least three independent experiments ($n = 3$), with each experiment performed in triplicate. Multiple group comparisons were conducted using one-way analysis of variance (ANOVA), followed by Tukey's post hoc test (GraphPad Prism, version 9). Statistical significance was established at $p < 0.05$.

2.3. Network pharmacology analysis

2.3.1. Collection of BA targets

The chemical structure of BA, including its SMILES, InChI, and SDF formats, was retrieved from the PubChem database (**Table 1**). Target prediction for BA was performed using multiple databases, including BATMAN-TCM (probability $\geq 80\%$), SuperPred (probability ≥ 0.7), SwissTargetPrediction (probability > 0.1), and PharmMapper (probability ≥ 0.7). The predicted targets were standardized using UniProt, and duplicates were removed to obtain a final list of BA-related targets.

2.3.2. Screening of T2DM-related targets

T2DM-related targets were retrieved from multiple databases, including CTD (score ≥ 80), OpenTargets (score ≥ 0.3), GeneCards (score ≥ 60), and DrugBank, using "T2DM" as the keyword. The retrieved targets were standardized, and duplicates were removed to obtain a final list of T2DM-related targets. The intersection between BA-related targets and T2DM-related targets was identified using the VennDiagram package in R (version 4.2.1), and the overlapping targets were considered potential therapeutic targets for BA in treating T2DM.

Table 1. List of databases.

Databases	URL
Genecards	https://www.genecards.org/
Drugbank	https://go.drugbank.com/
CTD	http://ctdbase.org/
Open Targets	https://www.opentargets.org/
SuperPred	https://prediction.charite.de/
SwissTargetPrediction	http://swisstargetprediction.ch/
BATMAN-TCM	http://bionet.ncpsb.org.cn/batman-tcm/index.php
PubChem	https://pubchem.ncbi.nlm.nih.gov/
PharmMapper	https://lilab-ecust.cn/pharmmapper/index.html

2.3.3. Construction of compound-target-disease network

The network mapping of the compound-target-disease relationship was facilitated by Cytoscape software (version 3.9.1). In this network, nodes stood for the bioactive compound BA and its associated targets, while the connections (edges) depicted the interplay between them. The Network Analyzer plugin was employed to examine the network's structural characteristics, and the degree centrality of each node was determined to highlight key target molecules.

2.3.4. Protein-protein interaction (PPI) network construction and analysis

The overlapping targets were integrated into the STRING database to build a protein-protein interaction (PPI) network. The species parameter was specified as "Homo sapiens" and interactions were filtered using a confidence threshold of 0.7 or higher. This network was subsequently imported into Cytoscape for in-depth examination. Nodes without connections were eliminated, and the network's structure was evaluated using the Network Analyzer plugin. Critical targets were pinpointed by assessing their degree, betweenness centrality (BC), and closeness centrality (CC) metrics.

2.3.5. GO and KEGG pathway enrichment analysis

Used clusterProfiler in R (v4.2.1) for GO and KEGG enrichment analyses. GO analysis included biological processes, molecular functions, and cellular components with $p < 0.05$ significance. KEGG analysis adhered to the same criteria. Key results, like top 20 GO terms and top 30 KEGG pathways, were visualized with bar charts and bubble plots.

2.3.6. Construction of compound-target-pathway-disease network

To uncover the mechanisms behind BA's actions, we developed a compound-target-pathway-disease network using Cytoscape. This cohesive network assembled critical compounds, targets, and pathways, offering a comprehensive understanding of BA's therapeutic approach, which is distinguished by its varied, multi-targeted, and multi-pathway action.

2.3.7. Molecular docking

Conducted molecular docking to confirm BA-target interactions. BA's 3D structure from PubChem and target proteins from PDB were prepared with PyMOL

(v2.6.0) and AutoDock Tools (v1.5.7). Docking performed with AutoDock Vina (v1.2.3), results visualized with PyMOL and Discovery Studio. Favorable binding is indicated by energies < -5.0 kcal/mol, strong binding by < -7.5 kcal/mol.

3. Result

3.1. Optimization of MGO-induced oxidative stress and assessment of BA cytotoxicity

The CCK-8 assay was used to determine the effects of MGO and BA on Ins-1 cell viability. As illustrated in **Figure 1A**, MGO treatment resulted in a dose- and time-dependent reduction in cell viability. At 1000 μM , MGO significantly impaired cell viability after 12 h, with a further decline to 8.02% after 48 h of incubation. Based on these results, 1000 μM MGO with a 12 h incubation period was selected for subsequent experiments to model oxidative stress, as this condition effectively induced cellular damage while maintaining a sufficient window for therapeutic intervention. In **Figure 1B**, BA treatment at concentrations up to 100 μM showed no significant cytotoxicity at 12 and 24 h, with cell viabilities of 97% and 110%, respectively. However, prolonged exposure to 100 μM BA for 48 h reduced cell viability to 63.56%, indicating potential toxicity at higher concentrations over extended periods. Based on these findings, BA concentrations of ≤ 50 μM were chosen for further experiments to ensure minimal cytotoxicity while maintaining therapeutic efficacy. These results establish 1000 μM MGO with a 12 h incubation as an effective condition for inducing oxidative stress and confirm that BA at ≤ 50 μM is safe for short-term treatments, providing a reliable framework for subsequent investigations into the protective effects of BA against MGO-induced cellular damage.

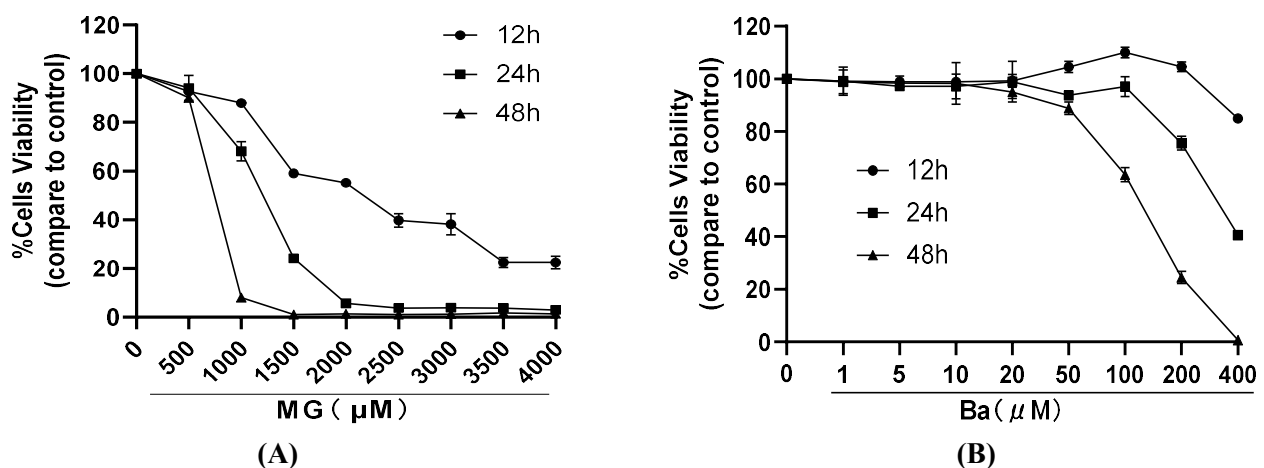


Figure 1. Effects of MGO and BA on Ins-1 cell viability. **(A)** Cell viability of Ins-1 cells treated with varying concentrations of BA (0–400 μM) for 12, 24, and 48 h, as assessed by the CCK-8 assay; **(B)** cell viability of Ins-1 cells treated with varying concentrations of MGO (0–4000 μM) for 12, 24, and 48 h. Data are presented as percentages relative to the untreated control group (mean \pm SD, $n = 6$).

3.2. Comparative analysis of BA treatment strategies against MGO-induced oxidative

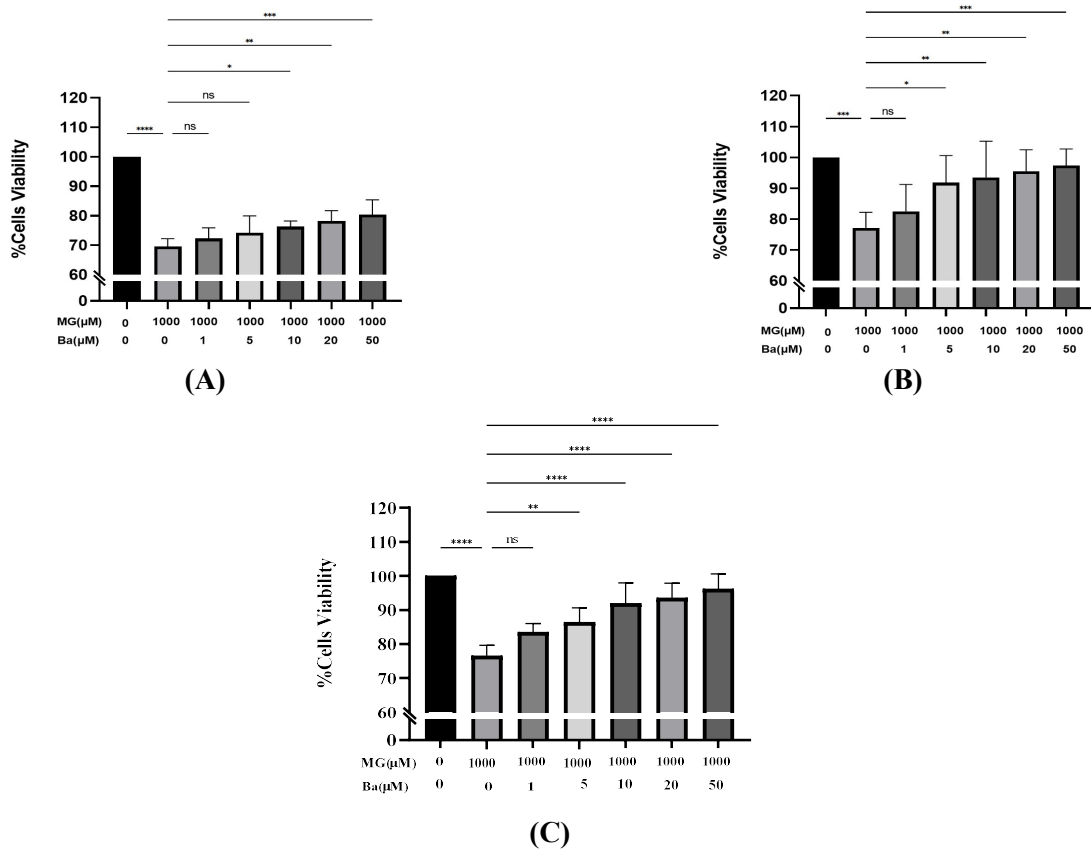


Figure 2. Effects of different BA treatment strategies on MGO-induced cytotoxicity in Ins-1 cells. **(A)** Cell viability following pretreatment with 1000 μM MGO for 12 h, followed by BA (0–50 μM) for an additional 12 h; **(B)** cell viability following pretreatment with varying concentrations of BA (0–50 μM) for 12 h, followed by 1000 μM MGO for another 12 h; **(C)** cell viability following co-treatment with 1000 μM MGO and BA (0–50 μM) for 12 h.

Note: Data are presented as percentages relative to the untreated control group (mean \pm SD, $n = 6$). * $P < 0.05$, ** $P < 0.01$, *** $P < 0.001$, **** $P < 0.0001$.

To evaluate the efficacy of BA in mitigating MGO-induced cytotoxicity, Ins-1 cells were subjected to three treatment strategies: (1) pretreatment with MGO followed by BA, (2) pretreatment with BA followed by MGO, and (3) co-treatment with MGO and BA. In the first strategy, pretreatment with 1000 μM MGO for 12 h followed by BA (0–50 μM) for an additional 12 h revealed that low concentrations of BA (1 μM) had no significant therapeutic effect, while medium to high concentrations (10–50 μM) dose-dependently restored cell viability, with 50 μM BA showing the most pronounced recovery (**Figure 2A**). In the second strategy, pretreatment with BA (0–50 μM) for 12 h prior to 1000 μM MGO exposure demonstrated that 1 μM BA provided no protection, whereas higher concentrations (10–50 μM) dose-dependently attenuated cytotoxicity, with 50 μM BA exhibiting the strongest protective effect (**Figure 2B**). The third strategy, involving co-treatment with 1000 μM MGO and BA (0–50 μM) for 12 h, showed that even low concentrations of BA (1 μM) provided some therapeutic benefit, with increasing efficacy at higher doses (10–50 μM). The 50 μM BA group achieved the highest cell viability, surpassing the other treatment strategies (**Figure**

2C). These results highlight the dose-dependent protective effects of BA, with co-treatment emerging as the most effective approach due to BA's immediate antioxidant and anti-apoptotic actions during MGO exposure.

3.3. Assessment of intracellular ROS levels in MGO-induced oxidative stress and BA intervention

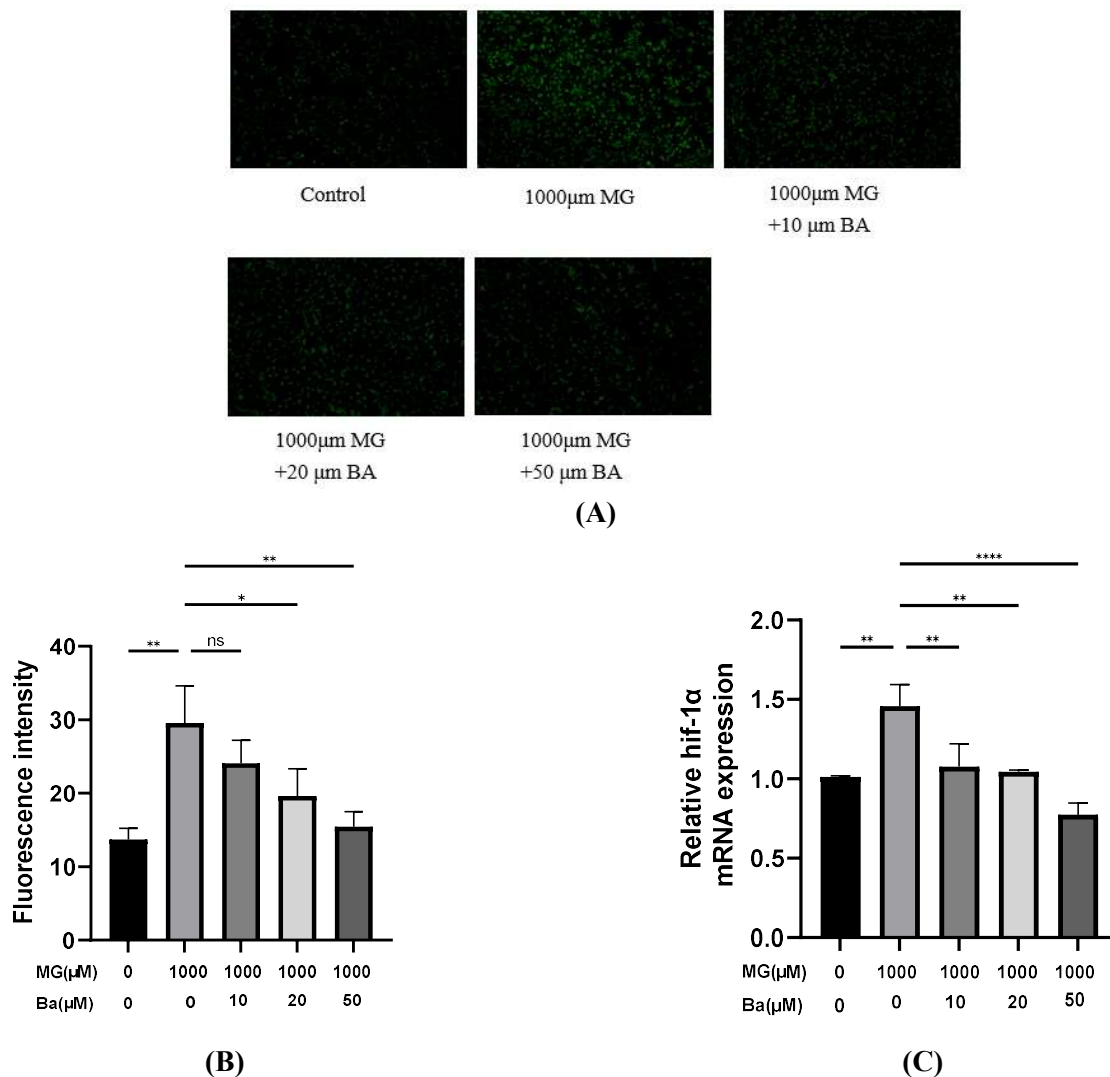


Figure 3. Effects of BA on intracellular ROS levels and HIF-1α expression in MGO-induced oxidative stress. **(A)** Representative fluorescence images of intracellular ROS levels in Ins-1 cells; **(B)** quantitative analysis of fluorescence intensity, reflecting intracellular ROS levels; **(C)** relative mRNA expression of HIF-1α in Ins-1 cells.

Note: Data are presented as mean ± SD ($n = 3$). * $P < 0.05$, ** $P < 0.01$, **** $P < 0.0001$.

To evaluate the effects of BA on MGO-induced oxidative stress, intracellular ROS levels were measured using fluorescence staining and quantitative analysis. **Figure 3A** illustrates the fluorescence images of ROS levels in Ins-1 cells under different treatment conditions. The control group exhibited minimal fluorescence, indicating low basal ROS levels. In contrast, cells treated with 1000 μM MGO displayed a marked increase in fluorescence intensity, confirming the induction of oxidative stress. Quantitative analysis of fluorescence intensity (**Figure 3B**) further

supported these observations. The MGO-treated group exhibited a significant increase in fluorescence intensity compared to the control group, indicating elevated ROS production. While co-treatment with 10 μM BA resulted in a slight reduction in ROS levels, this change was not statistically significant. However, treatment with 20 μM and 50 μM BA significantly attenuated oxidative stress, with the 50 μM BA group showing the most pronounced reduction in ROS levels. Statistical analysis revealed significant differences between the MGO-treated group and the groups co-treated with 20 μM and 50 μM BA, highlighting the dose-dependent antioxidant effects of BA.

In addition to ROS levels, the relative mRNA expression of HIF-1 α , a key transcription factor involved in cellular responses to oxidative stress, was also assessed (**Figure 3C**). The MGO-treated group exhibited a significant upregulation of HIF-1 α expression compared to the control group. Co-treatment with BA at 10 μM , 20 μM , and 50 μM progressively reduced HIF-1 α expression, with the 50 μM BA group showing the most significant reduction. These findings suggest that BA not only mitigates ROS production but also modulates the expression of HIF-1 α , further supporting its role in alleviating oxidative stress in T2DM.

4. β -galactosidase staining in MGO-induced senescence and BA treatment

To investigate the effects of BA on MGO-induced cellular senescence, β -galactosidase staining and P53 mRNA expression were assessed. **Figure 4A** presents the representative images of β -galactosidase staining in Ins-1 cells under different treatment conditions. The control group exhibited minimal staining, indicating low levels of cellular senescence. In contrast, cells treated with 1000 μM MGO displayed a significant increase in β -galactosidase-positive cells, confirming the induction of senescence. Co-treatment with BA at concentrations of 10 μM , 20 μM , and 50 μM progressively reduced the percentage of senescent cells, as evidenced by the decreasing intensity of blue staining. Notably, the 50 μM BA group showed the most significant reduction, with staining levels approaching those of the control group, suggesting a potent anti-senescence effect at higher BA concentrations. Quantitative analysis of β -galactosidase-positive cells (**Figure 4B**) further supported these observations. The MGO-treated group exhibited a significant increase in the percentage of senescent cells compared to the control group. Co-treatment with BA at 10 μM , 20 μM , and 50 μM resulted in a dose-dependent reduction in senescent cells, with the 50 μM BA group showing the most pronounced decrease. Statistical analysis indicated significant differences between the MGO-treated group and the groups co-treated with BA, underscoring the dose-dependent anti-senescence effects of BA.

In addition to β -galactosidase staining, the relative mRNA expression of P53, a critical regulator of cellular senescence, was assessed (**Figure 4C**). The MGO-treated group showed a significant upregulation of P53 expression compared to the control group. Co-treatment with BA at 10 μM , 20 μM , and 50 μM progressively reduced P53 expression, with the 50 μM BA group exhibiting the most significant reduction.

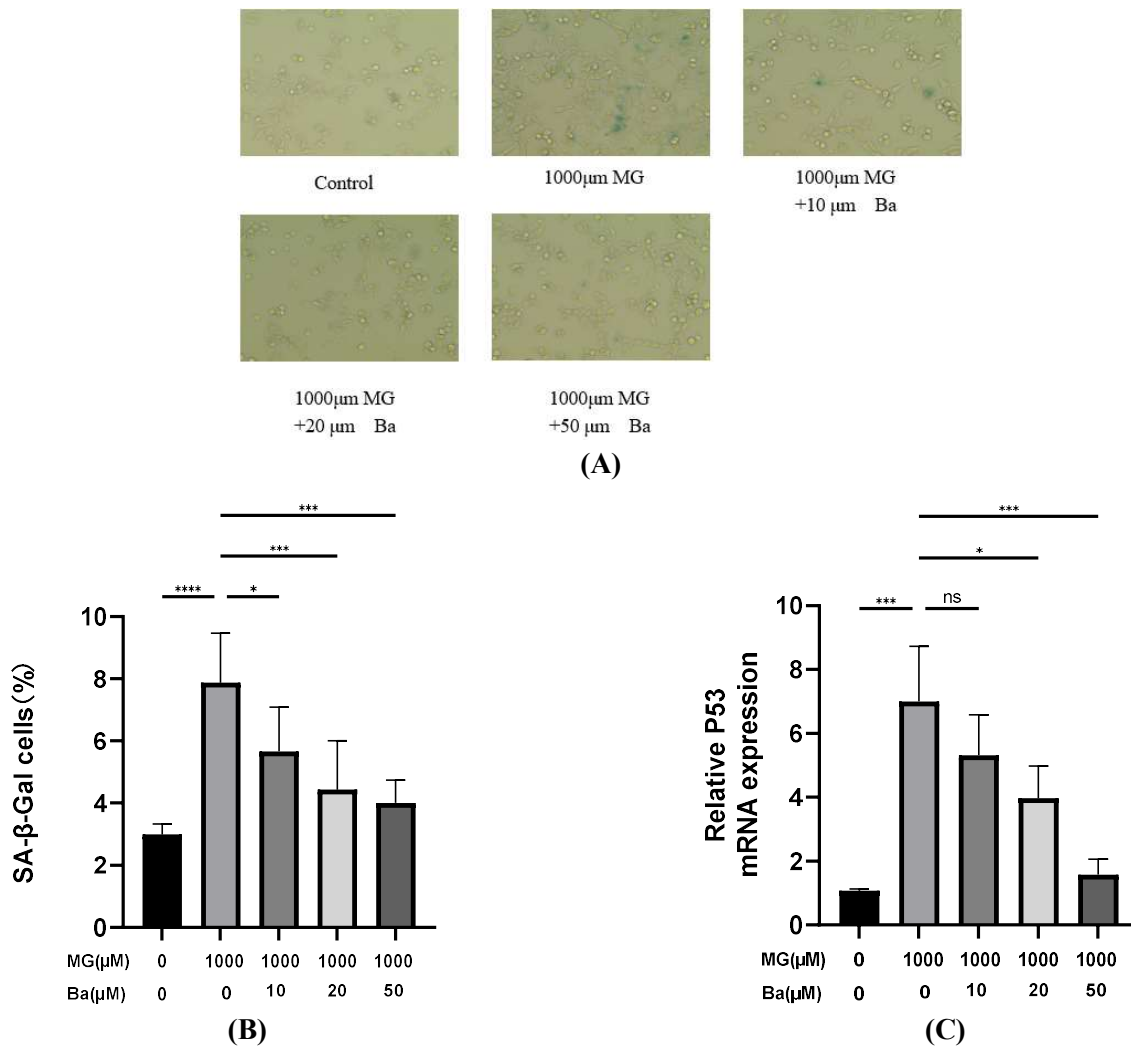


Figure 4. Influence of BA on MGO-triggered cellular senescence via β -galactosidase assay. **(A)** Microscopic images showing β -galactosidase staining in Ins-1 cells; **(B)** measurement of the percentage of cells positive for β -galactosidase activity relative to the total cell count; **(C)** mRNA expression of P53 in Ins-1 cells, with data represented as mean \pm standard deviation ($n = 3$).

Note: Statistical significance indicated by * $P < 0.05$, *** $P < 0.001$, **** $P < 0.0001$.

5. Flow cytometry analysis of apoptosis

To examine the effect of BA on apoptosis triggered by MGO, both flow cytometry and qPCR for genes linked to apoptosis were performed. **Figure 5A** reveals the flow cytometry outcomes, which illustrate the variation in apoptotic cell proportions based on the treatment applied. The control group displayed minimal levels of apoptosis, while the MGO-treated group experienced a notable upsurge in apoptotic cells, confirming the onset of apoptosis. Administration of BA at concentrations of 10 μ M, 20 μ M, and 50 μ M led to a progressive decline in the apoptotic cell count, with the 50 μ M BA dose yielding the most significant decrease. Statistical analysis demonstrated a marked distinction between the MGO-only group and those also receiving BA, emphasizing the dose-related inhibitory effect of BA on apoptosis.

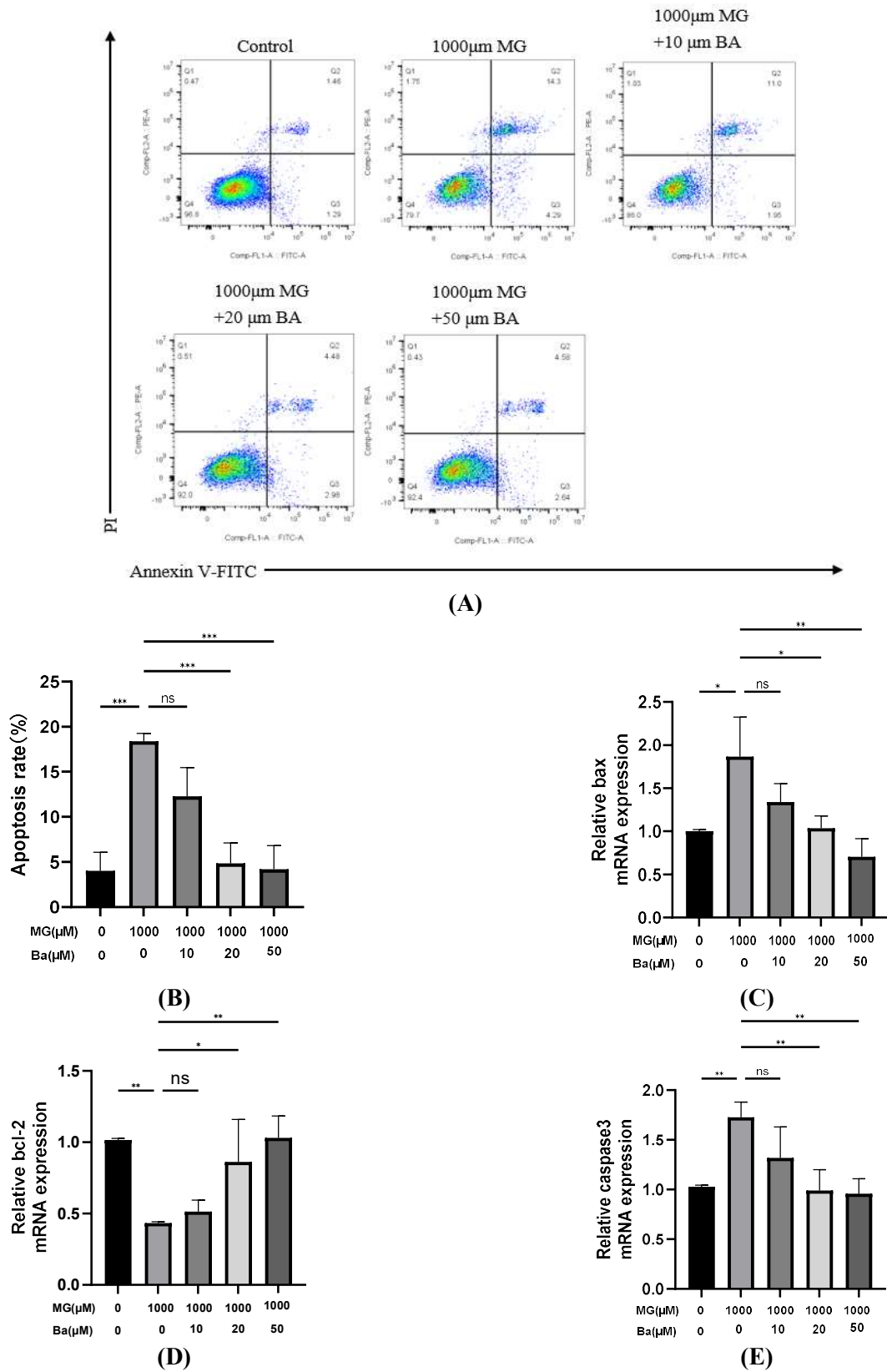


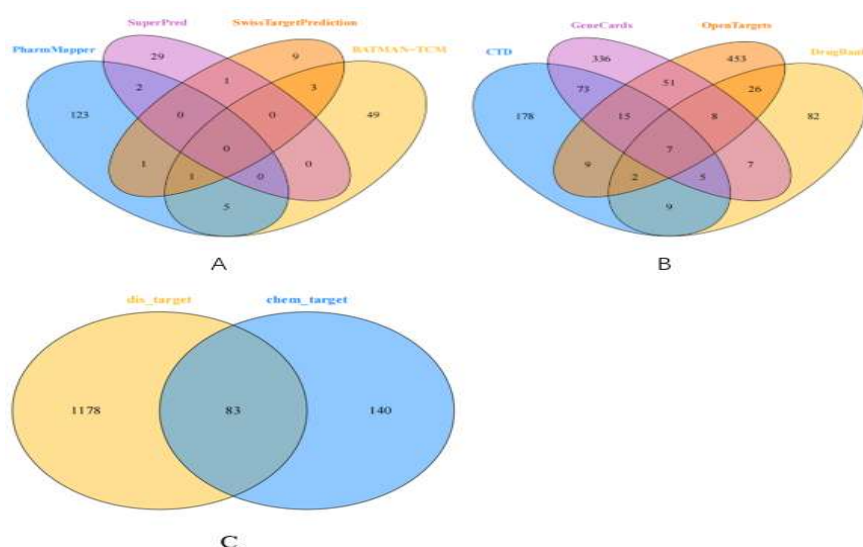
Figure 5. Assessment of BA's modulation on MGO-triggered apoptosis via flow cytometry. **(A and B)** Flow cytometric assessment of apoptotic populations in the Ins-1 cell culture, with apoptosis quantification achieved through Annexin V-FITC and propidium iodide (PI) staining; **(C–E)** mRNA expression ratios of Bax, Bcl-2, and Caspase-3 in Ins-1 cells.

Note: Data are represented as mean \pm standard deviation ($n = 3$). Statistical significance indicated by * $P < 0.05$, ** $P < 0.01$, *** $P < 0.001$.

In addition to flow cytometry, the relative mRNA expression of key apoptosis-related genes, including Bax, Bcl-2, and Caspase-3, was assessed (**Figure 5C–E**). The MGO-treated group exhibited a significant upregulation of pro-apoptotic genes (Bax and Caspase-3) and downregulation of the anti-apoptotic gene (Bcl-2) compared to the control group. Co-treatment with BA at 10 μ M, 20 μ M, and 50 μ M progressively modulated the expression of these genes, with the 50 μ M BA group showing the most significant changes. These results suggest that BA not only reduces apoptosis but also modulates the expression of key apoptosis-related genes, further supporting its role in mitigating apoptosis in T2DM.

6. Establishment of PPI network analysis

The PPI network analysis revealed 83 overlapping targets between BA and T2DM, as shown in the Venn diagram (**Figure 6C**). These targets were further analyzed to construct a compound-target-disease network (**Figure 6D**), which demonstrated that BA interacts with multiple targets, including Bax, Bcl-2, Caspase-3, and HIF-1 α , suggesting a multi-target mechanism of action. The STRING interaction map (**Figure 6E**) and PPI network (**Figure 6F**) highlighted the strong interconnectivity among the overlapping targets, with key hub proteins such as AKT1, EGFR, IL6, IL1B, TNF, and STAT3 playing central roles. These targets are involved in critical pathways related to oxidative stress, apoptosis, and inflammation, which are central to T2DM pathogenesis. The degree ranking plot (**Figure 6G**) further confirmed the importance of these hub targets, with AKT1 and STAT3 exhibiting the highest connectivity. These findings suggest that BA exerts its therapeutic effects by modulating a network of interconnected proteins, aligning with the multi-component and multi-target approach of traditional Chinese medicine. This comprehensive analysis provides valuable insights into the potential mechanisms underlying BA's protective effects against T2DM-related complications.



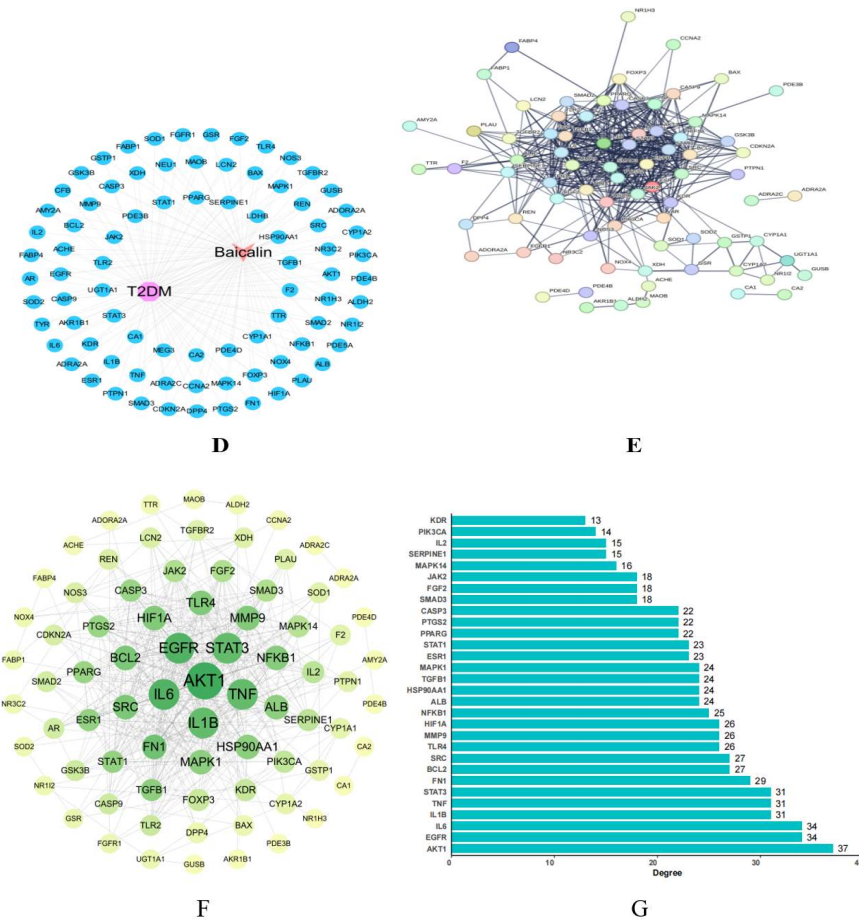


Figure 6. Protein-protein interaction (PPI) network analysis. **(A)** BA-related targets; **(B)** T2DM-related targets; **(C)** Venn diagram of the overlapping targets between BA and T2DM; **(D)** compound-target-disease network constructed using Cytoscape, illustrating the interactions between BA, its targets, and T2DM; **(E)** STRING interaction map of the overlapping targets, with edges representing protein-protein interactions (confidence score ≥ 0.7); **(F)** PPI network visualized using Cytoscape, highlighting key hub targets based on degree values; **(G)** bar plot ranking the core targets by their degree values, with AKT1, EGFR, IL6, IL1B, TNF, and STAT3 identified as the most highly connected targets.

7. GO and KEGG analysis

The GO enrichment analysis revealed that the 83 overlapping targets of BA and T2DM were significantly enriched in biological processes such as regulation of smooth muscle cell proliferation, wound healing, and cellular response to lipopolysaccharide (**Figure 7A**). In the molecular function category, targets were enriched in nitric-oxide synthase regulator activity and nuclear receptor activity, while cellular component analysis highlighted enrichment in serine protease inhibitor complex and caveola. These findings suggest that BA may modulate cellular processes related to inflammation, oxidative stress, and tissue repair, which are critical in T2DM pathogenesis.

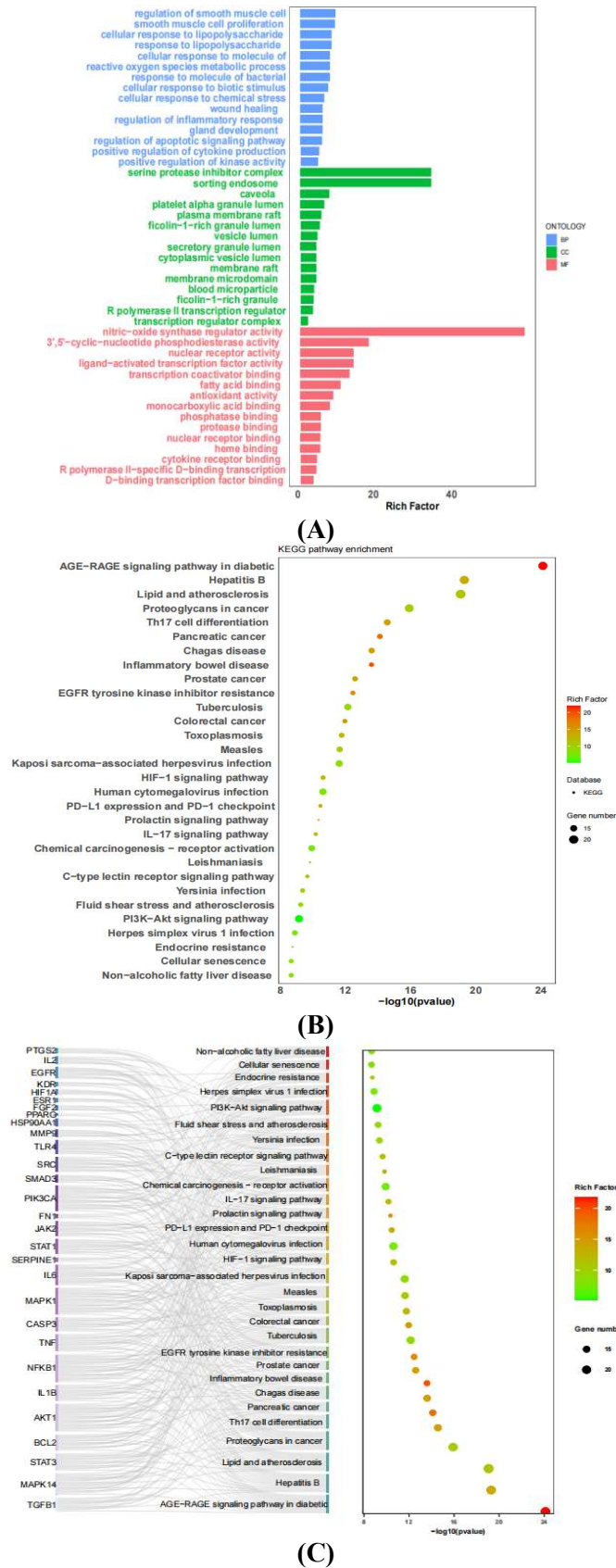


Figure 7. GO and KEGG pathway enrichment analysis. **(A)** Bar plots showing the top 20 significantly enriched GO terms in BP, MF, and CC categories ($p < 0.05$); **(B)** bubble plot displaying the top 30 significantly enriched KEGG pathways ($p < 0.05$). **(C)** Sankey bubble plot illustrating the relationships between key targets, top pathways, and their corresponding biological functions.

The KEGG pathway analysis identified 164 significantly enriched pathways ($p < 0.05$), with the top 30 pathways visualized in a bubble plot (**Figure 7B**). Key pathways included the AGE-RAGE signaling pathway in diabetic complications, Hepatitis B, Lipids and atherosclerosis, and the HIF-1 signaling pathway. These pathways are closely associated with T2DM progression, particularly in regulating oxidative stress, inflammation, and metabolic dysfunction. The Sankey bubble plot (**Figure 7C**) further elucidated the relationships between key targets (e.g., AKT1, STAT3, IL6) and their involvement in critical pathways, demonstrating how BA may exert its therapeutic effects through multi-target and multi-pathway mechanisms.

8. Construction of network

The compound-target-pathway-disease network (**Figure 8**) provides a comprehensive visualization of the multi-target, and multi-pathway mechanisms underlying BA's therapeutic effects in T2DM. The network highlights the interconnectedness of BA's targets and their involvement in key pathways related to oxidative stress, inflammation, and metabolic regulation. For example, AKT1 and STAT3 are central hubs connecting multiple pathways, suggesting their critical roles in mediating BA's effects. The network also demonstrates that BA's therapeutic actions are not limited to isolated targets or pathways but involve a synergistic interplay. This aligns with the holistic approach of traditional Chinese medicine, where BA exert their effects through complex, interconnected mechanisms.

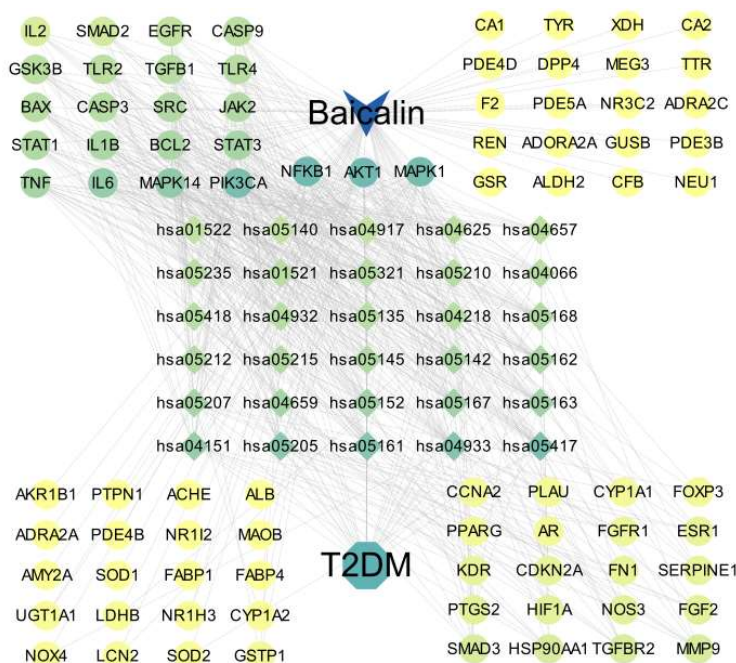


Figure 8. Compound-target-pathway-disease network.

9. Molecular docking analysis

To further elucidate the molecular interactions between BA and its potential targets, molecular docking analysis was performed. The heatmap (**Figure 9A**) illustrates the binding affinities (expressed as binding energies in kcal/mol) of BA with

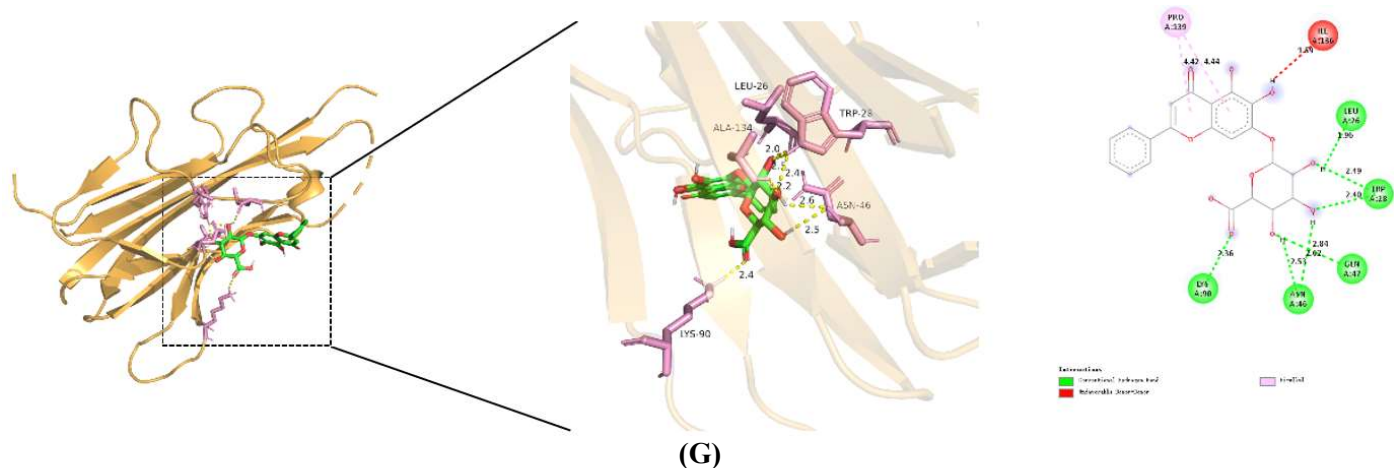


Figure 9. BA's association with essential target proteins. **(A)** Heatmap illustrating the docking potentials of prime compounds versus core targets; **(B–G)** close-up renderings of BA's molecular interface with individual targets: AT1-1, Bcl-2, EGFR, IL-1B, SRC, and TNF, in sequence.

10. Discussion

The present study investigated the therapeutic potential of BA, a bioactive flavonoid derived from *Scutellaria baicalensis*, in mitigating oxidative stress, cellular senescence, and apoptosis in an MGO-induced diabetic cell model. By integrating cellular experiments, network pharmacology, and molecular docking, we elucidated the multi-target mechanisms underlying BA's protective effects in T2DM. Our findings demonstrate that BA significantly improves cell viability, reduces ROS levels, and attenuates cellular senescence and apoptosis in Ins-1. Furthermore, network pharmacology and molecular docking analyses revealed that BA interacts with key targets such as HIF-1 α , Bax, Bcl-2, Caspase-3, AKT1, and PIK3R1, highlighting its multi-target therapeutic potential. This comprehensive approach not only confirmed BA's protective effects but also uncovered novel molecular pathways and targets, providing a deeper understanding of its mechanisms of action.

Cellular senescence, characterized by irreversible cell cycle arrest, is a key feature of T2DM pathogenesis [27]. Senescent β -cells lose their functional capacity and contribute to the decline in insulin production. In this study, MGO treatment significantly increased the percentage of senescent Ins-1 cells, as evidenced by β -galactosidase staining. BA co-treatment, particularly at higher concentrations, dose-dependently reduced cellular senescence, with the 50 μ M BA group showing the most significant reduction. The anti-senescence effects of BA were further supported by the downregulation of P53, a critical regulator of cellular senescence. These findings suggest that BA not only protects β -cells from oxidative stress but also prevents cellular senescence, thereby preserving their functional capacity. This is particularly important in the context of T2DM, where the loss of functional β -cells contributes to disease progression. Previous studies have shown that cellular senescence in β -cells is regulated by pathways such as the p53/p21 and p16INK4a/Rb pathways [28], which are activated under conditions of chronic hyperglycemia and oxidative stress. BA's ability to modulate these pathways, as suggested by our network pharmacology analysis, aligns with its anti-senescence effects. For instance, studies have demonstrated that natural compounds like resveratrol and quercetin can delay cellular

senescence by modulating these pathways, and our findings suggest that BA may act through similar mechanisms [29].

The programmed cell death of Ins-1 cells, a key feature of type 2 diabetes mellitus (T2DM), is primarily triggered by oxidative stress, chronic inflammation, and impaired mitochondrial function. Using flow cytometry, we observed that exposure to MGO markedly elevated apoptosis in Ins-1 cells, whereas the addition of BA in varying doses effectively curbed this process in a dose-dependent manner. Further evidence of BA's anti-apoptotic properties emerged through its influence on critical genes tied to cell death, such as Bax, Bcl-2, and Caspase-3. Specifically, BA suppressed the activity of pro-apoptotic genes (Bax and Caspase-3) while boosting the expression of the anti-apoptotic gene Bcl-2, indicating its role in blocking the intrinsic apoptotic pathway. These results align with earlier research highlighting BA's protective effects against apoptosis across diverse cell types, including neurons, heart muscle cells, and liver cells. By safeguarding β -cell survival and functionality, BA holds promise in supporting insulin production and glucose regulation—both essential for T2DM management. The intrinsic apoptotic pathway, governed by the Bcl-2 protein family, remains a well-documented driver of β -cell demise in diabetes.

Oxidative stress is a central pathogenic mechanism in T2DM, contributing to β -cell dysfunction, insulin resistance, and the development of diabetic complications. In this study, we observed that MGO-induced oxidative stress significantly increased intracellular ROS levels in Ins-1 cells, consistent with previous reports that hyperglycemia exacerbates ROS production through mitochondrial dysfunction and advanced glycation end products (AGEs) formation. BA treatment, particularly at higher concentrations (20 μ M and 50 μ M), effectively reduced ROS levels in a dose-dependent manner. This antioxidant effect aligns with BA's known ability to modulate the Nrf2/ARE pathway, which enhances cellular antioxidant defenses. Our findings are consistent with studies showing that BA reduces oxidative stress in various disease models, including diabetic nephropathy and cardiovascular diseases. The reduction in ROS levels by BA not only protects β -cells from oxidative damage but also mitigates downstream effects such as inflammation and apoptosis, which are critical in T2DM progression. The Nrf2/ARE pathway is a key regulator of cellular antioxidant responses, and its activation has been shown to protect β -cells from oxidative stress-induced damage. Other studies have demonstrated that natural compounds like sulforaphane and berberine can activate the Nrf2 pathway, leading to reduced oxidative stress and improved β -cell function. Our results suggest that BA may act through a similar mechanism, further supporting its potential as a therapeutic agent for T2DM.

In addition, chronic oxidative stress not only drives cellular damage through direct ROS-mediated cytotoxicity but also perturbs cytoskeletal dynamics, a critical determinant of β -cell structure and function. Oxidative insults disrupt actin polymerization and microtubule stability, leading to cytoskeletal disorganization that impairs insulin granule trafficking, cell adhesion, and mechanosignaling. This cytoskeletal dysfunction exacerbates β -cell secretory defects and promotes apoptosis, as cytoskeletal integrity is essential for maintaining insulin-producing capacity. Our study demonstrates that BA mitigates oxidative stress by reducing ROS levels and inhibiting HIF-1 α -mediated apoptotic pathways. Additionally, BA's modulation of

integrin-MAPK signaling—critical regulators of cytoskeletal dynamics—and potential interactions with cytoskeletal proteins (e.g., actin-binding proteins) may imply a hypothetical dual protective mechanism. By reducing oxidative stress, BA might indirectly support cytoskeletal integrity, while direct engagement with cytoskeletal components could potentially stabilize cellular architecture. This combined action may contribute to restoring β -cell mechanical phenotypes, thereby enhancing insulin secretion and survival in T2DM. Although direct experimental validation is needed, these observations suggest BA's potential as a multi-targeted agent addressing both redox imbalance and cytoskeletal dysfunction in diabetes.

Network pharmacology analysis identified 83 overlapping targets between BA and T2DM, including key proteins involved in oxidative stress, apoptosis, and inflammation pathways. The compound-target-disease network highlighted the interconnectedness of BA's targets, with AKT1, STAT3, and HIF-1 α emerging as central hubs. These findings align with the known roles of these proteins in T2DM pathogenesis. For example, AKT1 is a key regulator of insulin signaling and cell survival, while STAT3 and HIF-1 α are involved in inflammation and hypoxia responses, respectively. The strong interconnectivity among these targets suggests that BA exerts its therapeutic effects through a synergistic modulation of multiple pathways, consistent with the holistic approach of traditional Chinese medicine. The identification of these targets not only validates the findings from our cellular experiments but also provides a roadmap for future research into the mechanisms of BA and other natural compounds. Molecular docking further validated the interactions between BA and its potential targets, with binding energies ranging from -7.30 to -10.54 kcal/mol. Notably, BA exhibited the highest binding affinity with AKT1, achieving a binding energy of -10.54 kcal/mol, suggesting a highly stable interaction. Other targets, including HIF-1 α , Bcl-2, and Caspase-3, also showed significant binding affinities, further supporting BA's potential to modulate multiple pathways involved in T2DM pathogenesis. These results provide mechanistic insights into BA's multi-target action and highlight its potential as a therapeutic candidate for T2DM. The strong binding affinities observed in the docking analysis further validate BA's role in modulating key pathways, supporting its development as a therapeutic candidate. The identification of these interactions also opens up new avenues for the development of BA derivatives or combination therapies that could enhance its therapeutic efficacy.

The findings of this study have important implications for the development of BA-based interventions for T2DM. By targeting multiple pathways involved in oxidative stress, cellular senescence, and apoptosis, BA offers a comprehensive approach to managing T2DM and its complications. The dose-dependent effects observed in this study suggest that optimizing the dosage of BA is critical for maximizing its therapeutic benefits while minimizing potential cytotoxicity. Future studies should explore the pharmacokinetics and pharmacodynamics of BA in animal models and clinical trials to further validate its efficacy and safety. Additionally, the integration of network pharmacology and molecular docking provides a valuable framework for identifying novel therapeutic targets and pathways, which can be applied to other natural products and complex diseases.

11. Conclusion

The research findings validate that BA effectively counters MGO-mediated oxidative stress, cellular aging, and apoptosis in Ins-1 cells via a strategic, multi-pronged intervention. The convergence of cellular studies, network pharmacology, and molecular docking approaches has illuminated the therapeutic potential of BA in the management of T2DM. The results propose BA as a promising multi-target therapeutic agent for treating T2DM and associated conditions, providing a roadmap for subsequent clinical investigation and the advancement of BA-focused therapeutic strategies. Deciphering the molecular underpinnings of BA's efficacy strengthens natural product research and highlights the importance of an interdisciplinary research paradigm in drug innovation. The acquired knowledge not only enhances our comprehension of BA's action but also paves the way for innovative therapeutic approaches to combat T2DM and similar metabolic ailments.

Author contributions: Conceptualization, XZ; methodology, CG and XZ; software, YY and YW; validation, YW and HZ; formal analysis, XZ and ZW; investigation, CG and HZ; resources, JC and FL; data curation, ZW and HZ; writing—original draft, XZ; writing—review and editing, ZL and MG; visualization, YY and ZW; supervision, JC and FL; project administration, JC and FL; funding acquisition, JC and FL. All authors have read and agreed to the published version of the manuscript.

Funding: This work was supported by the National Natural Science Foundation of China (NSFC) Regional Fund (No. 82460874); the Guangxi Natural Science Foundation General Program (No. 2024GXNSFAA010354); and the Innovation Team Project for High-Level Talent Cultivation of Guangxi University of Chinese Medicine (No. 2022B007).

Ethical approval: Not applicable.

Informed consent statement: Not applicable.

Conflict of interest: The authors declare no conflict of interest.

References

1. Kleibert M, Tkacz K, Winiarska K, et al. The role of hypoxia-inducible factors 1 and 2 in the pathogenesis of diabetic kidney disease. *Journal of Nephrology*. 2024; 38(1): 37-47. doi: 10.1007/s40620-024-02152-x
2. Cheloi N, Asgari Z, Ershadi S, et al. Comparison of Body Mass Index, Energy and Macronutrient Intake, and Dietary Inflammatory Index Between Type 2 Diabetic and Healthy Individuals. *Journal of Research in Health Sciences*. 2024; 25: e00639. doi: 10.34172/jrhs.2025.174
3. Zhou X, Xu Z, You Y, et al. Subcutaneous device-free islet transplantation. *Frontiers in Immunology*. 2023; 14. doi: 10.3389/fimmu.2023.1287182
4. Pasupuleti P, Suchitra MM, Bitla AR, et al. Attenuation of Oxidative Stress, Interleukin-6, High-Sensitivity C-Reactive Protein, Plasminogen Activator Inhibitor-1, and Fibrinogen with Oral Vitamin D Supplementation in Patients with T2DM having Vitamin D Deficiency. *Journal of Laboratory Physicians*. 2021; 14(02): 190-196. doi: 10.1055/s-0041-1742285
5. Lee H, Kim SY, Lim Y. Lespedeza bicolor extract supplementation reduced hyperglycemia-induced skeletal muscle damage by regulation of AMPK/SIRT/PGC1 α -related energy metabolism in type 2 diabetic mice. *Nutrition Research*. 2023; 110: 1-13. doi: 10.1016/j.nutres.2022.12.007
6. Zhu J, Hu Z, Luo Y, et al. Diabetic peripheral neuropathy: pathogenetic mechanisms and treatment. *Frontiers in Endocrinology*. 2024; 14. doi: 10.3389/fendo.2023.1265372

7. Fan Q, Feng S, Chen J, et al. An Association between Bilirubin and Diabetic Retinopathy in Patients with Type 2 Diabetes Mellitus: An Effect Modification by Nrf2 Polymorphisms. *Current Diabetes Reviews*. 2024; 21. doi: 10.2174/0115733998327164240923070313
8. Sun R, Han M, Liu Y, et al. Trpc6 knockout protects against renal fibrosis by restraining the CN-NFAT2 signaling pathway in T2DM mice. *Molecular Medicine Reports*. 2023; 29(1). doi: 10.3892/mmr.2023.13136
9. Shah A, Isath A, Aronow WS. Cardiovascular complications of diabetes. *Expert Review of Endocrinology & Metabolism*. 2022; 17(5): 383-388. doi: 10.1080/17446651.2022.2099838
10. Sharif H, Akash MSH, Rehman K, et al. Pathophysiology of atherosclerosis: Association of risk factors and treatment strategies using plant-based bioactive compounds. *Journal of Food Biochemistry*. 2020; 44(11). doi: 10.1111/jfbc.13449
11. Ting Hao W, Huang L, Pan W, et al. Antioxidant glutathione inhibits inflammation in synovial fibroblasts via PTEN/PI3K/AKT pathway: An in vitro study. *Archives of Rheumatology*. 2021; 37(2): 212-222. doi: 10.46497/archrheumatol.2022.9109
12. Wu J, Deng L, Yin L, et al. Curcumin promotes skin wound healing by activating Nrf2 signaling pathways and inducing apoptosis in mice. *Turkish Journal of Medical Sciences*. 2023; 53(5): 1127-1135. doi: 10.55730/1300-0144.5678
13. Zhang HN, Zhang M, Tian W, et al. Canonical transient receptor potential channel 1 aggravates myocardial ischemia-and-reperfusion injury by upregulating reactive oxygen species. *Journal of Pharmaceutical Analysis*. 2023; 13(11): 1309-1325. doi: 10.1016/j.jpha.2023.08.018
14. Das N, Mukherjee S, Das A, et al. Intra-tumor ROS amplification by melatonin interferes in the apoptosis-autophagy-inflammation-EMT collusion in the breast tumor microenvironment. *Heliyon*. 2024; 10(1): e23870. doi: 10.1016/j.heliyon.2023.e23870
15. Zhang J, Li W, Li H, et al. Selenium-Enriched Soybean Peptides as Novel Organic Selenium Compound Supplements: Inhibition of Occupational Air Pollution Exposure-Induced Apoptosis in Lung Epithelial Cells. *Nutrients*. 2023; 16(1): 71. doi: 10.3390/nu16010071
16. Ma X, Jiao J, Aierken M, et al. Hypoxia Inducible Factor-1 α Through ROS/NLRP3 Pathway Regulates the Mechanism of Acute Ischemic Stroke Microglia Scorching Mechanism. *Biologics: Targets and Therapy*. 2023; 17: 167-180. doi: 10.2147/btt.s444714
17. Wang S, Wu X, Wang H, et al. Role of FBXL5 in redox homeostasis and spindle assembly during oocyte maturation in mice. *The FASEB Journal*. 2023; 37(8). doi: 10.1096/fj.202300244rr
18. Xu C, Hu L, Zeng J, et al. *Gynura divaricata* (L.) DC. promotes diabetic wound healing by activating Nrf2 signaling in diabetic rats. *Journal of Ethnopharmacology*. 2024; 323: 117638. doi: 10.1016/j.jep.2023.117638
19. Barillaro M, Schuurman M, Wang R. β 1-Integrin—A Key Player in Controlling Pancreatic Beta-Cell Insulin Secretion via Interplay with SNARE Proteins. *Endocrinology*. 2022; 164(1). doi: 10.1210/endo/bqac179
20. Cai W, Zhang Y, Jin W, et al. Procyanidin B2 ameliorates the progression of osteoarthritis: An in vitro and in vivo study. *International Immunopharmacology*. 2022; 113: 109336. doi: 10.1016/j.intimp.2022.109336
21. Yu H, Zhou D, Wang W, et al. Protective effect of baicalin on oxidative stress injury in retinal ganglion cells through the JAK/STAT signaling pathway in vitro and in vivo. *Frontiers in Pharmacology*. 2024; 15. doi: 10.3389/fphar.2024.1443472
22. Chen Y, Bao S, Wang Z, et al. Baicalin promotes the sensitivity of NSCLC to cisplatin by regulating ferritinophagy and macrophage immunity through the KEAP1-NRF2/HO-1 pathway. *European Journal of Medical Research*. 2024; 29(1). doi: 10.1186/s40001-024-01930-4
23. Cao Z, Ma N, Shan M, et al. Baicalin Inhibits FIPV Infection In Vitro by Modulating the PI3K-AKT Pathway and Apoptosis Pathway. *International Journal of Molecular Sciences*. 2024; 25(18): 9930. doi: 10.3390/ijms25189930
24. Li Y, Zhang Y, Huang C, et al. Baicalin improves neurological outcomes in mice with ischemic stroke by inhibiting astrocyte activation and neuroinflammation. *International Immunopharmacology*. 2025; 149: 114186. doi: 10.1016/j.intimp.2025.114186
25. Lee II, Chao CY, Yang YC, et al. Huang Lian Jie Du Tang attenuates paraquat-induced mitophagy in human SH-SY5Y cells: A traditional decoction with a novel therapeutic potential in treating Parkinson's disease. *Biomedicine & Pharmacotherapy*. 2021; 134: 111170. doi: 10.1016/j.biopha.2020.111170
26. Wang Y, Zhang J, Zhang B, et al. Modified Gegen Qinlian decoction ameliorated ulcerative colitis by attenuating inflammation and oxidative stress and enhancing intestinal barrier function in vivo and in vitro. *Journal of Ethnopharmacology*. 2023; 313: 116538. doi: 10.1016/j.jep.2023.116538

27. Wen Y, Zhang X, Liu H, et al. SGLT2 inhibitor downregulates ANGPTL4 to mitigate pathological aging of cardiomyocytes induced by type 2 diabetes. *Cardiovascular Diabetology*. 2024; 23(1). doi: 10.1186/s12933-024-02520-8
28. Wang Z, Li L, Liao S, et al. Canthaxanthin Attenuates the Vascular Aging or Endothelial Cell Senescence by Inhibiting Inflammation and Oxidative Stress in Mice. *Frontiers in Bioscience-Landmark*. 2023; 28(12). doi: 10.31083/j.fbl2812367
29. Liu HM, Cheng MY, Xun MH, et al. Possible Mechanisms of Oxidative Stress-Induced Skin Cellular Senescence, Inflammation, and Cancer and the Therapeutic Potential of Plant Polyphenols. *International Journal of Molecular Sciences*. 2023; 24(4): 3755. doi: 10.3390/ijms24043755